Supplementary data

Biodegradation of 2,4-dinitrotoluene with *Rhodococcus pyridinivorans* NT2: Characteristics, kinetic modeling, physiological responses and metabolic pathway

Debasree Kundu, Chinmay Hazra, Ambalal Chaudhari*

School of Life Sciences, North Maharashtra University, Jalgaon, Maharashtra, India

*Corresponding author. School of Life Sciences, North Maharashtra University, P.B. No. 80, Jalgaon 425 001, India. Tel.: +91 257 2257425. E-mail: ambchasls@gmail.com; ambchasls@yahoo.com (Ambalal Chaudhari)

Effect of operational parameters on growth of 2,4-DNT degrading bacteria

To study the effect of age of inoculum on the rate of 2,4-DNT degradation at 100 mg l^{-1}, cell biomass was raised in different flasks to obtain inoculum of various age (12, 18, 24, 48 and 96 h).

To study the effect of inoculum size on the rate of 2,4-DNT degradation at 100 mg l^{-1}, 100 ml MSB medium in 500 ml Erlenmeyer flask was incubated with various cell densities (0.2 - 2.0 mg dry cell weight l^{-1}) at 30^{o}C for 24 h. Aliquots were withdrawn at regular intervals for estimation of residual 2,4-DNT.

Since prior exposure history significantly affects the degradation pattern, enhancement of degradation rate by pre-exposed cells were investigated. The acclimatization of the isolate was done by incrementally increasing their exposure to 2,4-DNT. Initially, it was grown in MSB medium containing 20 mg l^{-1} (*i.e.*, 0.1 mM) of 2,4-DNT (as the only carbon, nitrogen and energy source) and incubated at 30 ^{o}C under shaking at 120 rpm upto 24 h. The cells were harvested when the OD_{600} reached 1.2-1.5, washed twice with MSB, and inoculated into MSB containing 0.5 mM of 2,4-DNT. This same protocol was followed for next successive steps with increasing 2,4-DNT concentration (0.7, 1.0, 1.2, 1.4, 1.6, 1.8 and 2.0 mM). The inoculum used for each batch run was taken from the culture grown in the previous run. The culture not exposed to 2,4-DNT was run simultaneously to serve as a control.

To find out optimal values of pH and temperature on 2,4-DNT degradation, 18 h-old culture of NT2 strain was inoculated in MSB media with an inoculum density of 1.6 mg cdw l^{-1} over a pH range of 5-9 and temperature range of 20-50 ^{o}C.

Kinetics models: theoretical background

In this work, since the flasks were covered with six layer gauzes, it was assumed that the aeration provided by shaking the flasks was able to keep the oxygen concentration sufficient and not limited; hence the influence of oxygen was not considered. Thus, the *Rhodococcus* sp. growth rate and degradation rate of 2,4-DNT were only limited by substrate concentration at fixed initial pH, temperature and shaking rate.

Modeling any biodegradation process involves relating the specific growth rate of the biomass to the consumption rate of the substrate (contaminant). For this purpose, specific growth rates of strain NT2 at different concentrations of 2,4-DNT were calculated as per the following equation:[1]

$$\mu = \frac{1}{X}\frac{dX}{dt} \tag{1}$$

where, X is biomass concentration (mg l^{-1}) at time t (h) and μ is the specific growth rate (h^{-1}).

In the literature, two approaches are mostly encountered for representing the kinetics of bacterial growth on substrates. According to one, substrates are considered non-inhibitory compounds and so are represented by the Monod model which can be expressed as given below:

$$\mu = \frac{\mu_{max} S}{K_s + S} \tag{2}$$

The other view considers the substrates to be growth inhibitory compounds. Of the kinetics models describing the growth kinetics of inhibitory compound, Haldane's model is widely studied due to its mathematical simplicity and wide acceptance for representing the growth kinetics of inhibitory substrates. The Haldane's or Andrews inhibitory growth kinetics has the same form and can be expressed as:

$$\mu = \frac{\mu_{max} S}{K_s + S + (S^2/K_i)} \quad (3)$$

where, μ_{max} is the maximum specific growth rate (h^{-1}); K_s is the half saturation coefficient (mg l^{-1}); K_i is the inhibition constant for cell growth (mg l^{-1}). An extended Monod type model originally proposed by Han-Levenspiel has also shown to be efficient in explaining the growth of the microorganism at different concentrations of substrate:[2,3]

$$\mu = \frac{\mu max [1-S/Sm]n}{Ks + S-[1-S/Sm]m} \quad (4)$$

where, S_m is the critical inhibitor concentration above which reactions stops and n and m are empirical constants. Also, Aiba-Edwards model[4] accounts for inhibitory effect of substrate concentration on microbial growth:

$$\mu = \mu_{max} \frac{S}{K_s + S} \exp(-S/K_i)$$

However, in some instances a stationary or zero-order growth phase is present between exponential and decay growth phase and hence, inappropriate. To overcome this phenomenon, Wayman and Tseng[5] developed a discontinuous model (Eqs. 5a-5c) which exhibits exponential, stationary, and decay phase, showing a sharp, linear drop in microbial activity when substrate concentration go above a characteristic threshold concentration (S_θ), thus leading to a complete decay of bacteria at a terminal concentration (S_i).

$$\mu = \mu max \frac{S}{Ks + S} \;,\; S \leq S\theta \quad (5a)$$

$$\mu = \mu max \frac{S}{Ks + S} - i\,(S - S\theta) \;,\; S\theta < S \leq Si \quad (5b)$$

$$\mu = 0 \;,\; S \geq Si \quad (5c)$$

A modified Wayman and Tseng model was developed by Alagappan and Cowan[6] to fit the observed growth data showing an apparent Andrew type inhibition, i.e., a minor drop in activity at moderate substrate concentration followed by a rapid loss of activity at higher concentrations. This new model is represented as Eqs. 6a-6c.[7]

$$\mu = \mu max \frac{S}{Ks + S + S2/Ki}, \quad S \leq S\theta \tag{6a}$$

$$\mu = \mu max \frac{S}{Ks + S + S2/Ki} - i\,(S - S\theta), \quad S\theta \leq \; \leq \tag{6b}$$

$$\mu = 0, \; S \geq Si \tag{6c}$$

The cell mass yield coefficient (dry weight of biomass/weight of substrate) was estimated by linearizing cell mass density increase with consumption of NTs as is given below:[8]

$$Y = \frac{X - X_0}{S_0 - S} \tag{7}$$

where, X_0 and X are the initial and final biomass concentration at the end of the culture with corresponding substrate concentrations S_0 and S.

The variation of biomass yield as a function of 2,4-DNT concentration can be further rationalized by a material balance on substrate consumption:

$$\frac{1}{Y} = \frac{1}{YC} + \frac{1}{YE} \tag{8}$$

where, Y_C represents the theoretical yield of cell mass on 2,4-DNT, Y_E corresponds to the yield of cell mass on 2,4-DNT consumed for energy, and Y is the observed cell yield on 2,4-DNT.

Total cellular fatty acid composition analysis

The alteration in total cellular fatty acid composition as a response was determined by fatty acid methyl esters (FAMEs) analysis following exposure of the selected strain to 2 mM of 2,4-DNT. Cells were harvested at 0 h and 72 h and FAMEs were prepared sequentially by saponification, methylation and extraction. The samples were analysed by gas chromatography (model: 6850 Series II, Agilent, USA) equipped with a flame ionization detector and 30 m Rtx®-5 (fused silica) capillary column (Restek, Bellefonte, PA) as described by Rajan *et al*.[9] Fatty acid profiles were identified with Sherlock software version 6.0B (RTSBA6 library version 6.00, MIDI). The peaks were automatically named and quantitated by the system.

Cell morphology by scanning electron microscopy (SEM) and morphometric analysis

For high-resolution field emission scanning electron microscopy (FESEM), cells from culture flasks containing 2,4-DNT (2 mM) were harvested at different time intervals (0, 12, 24 and 48 h), washed twice with ice-cold phosphate buffer (10 mM, pH 7.0) and fixed with mixture of 2.5% (v/v) glutaraldehyde. The cells were then washed twice with ice-cold phosphate buffer to remove excess of the fixative reagents, followed by a graded water-ethanol series (30%, 50%, 70%, 90%, and absolute ethanol) treatment. Subsequently, specimens in 100% ethanol were gold-coated for 15 min using a sputter-coater (E-102, Hitachi, Japan). The average thickness of the gold film applied to the samples was approximately 15 nm. Imaging was performed in a S-4800 SEM (Hitachi, Japan) with secondary electrons (SE) at 20 kV acceleration voltage and at room temperature. The cell dimensions of individual cylindrical bodies were directly measured from the SEM photographs to calculate the cell volume and the surface area by the following:[10-12]

$$Volume\ (\mu m3) = \frac{\pi W2L}{4} + \frac{\pi W2r}{3}$$

(9)

$$Surface\ area\ (\mu m2) = \pi WL + 4\pi r^2$$

(10)

where *W* is the width, *L* is the length, and *r* is the equatorial radius of the spheroid caps at both ends of the cylindrical cells. The average cellular volumes and surface area were calculated using 30 individual bacteria per population. Cells undergoing division or showing deformations/depressions were not considered.

Elucidation of uptake mechanism: surface activity tests

Unless stated otherwise, 2,4-DNT (2 mM) grown cells were harvested at end of log phase, centrifuged and culture supernatant of strain NT2 was used. Fresh uninoculated MSB (with 2,4-DNT) medium and 1% SDS were used as negative and positive controls, respectively.

For Parafilm M test, 1 ml of methylene blue [0.1% (w/v)] was added to 20 µl of cell-free culture supernatant. The resulting mixture was spotted onto a piece of Parafilm M sheet as a hydrophobic surface and photographed after 5 min. The methylene blue was added solely for visualization purposes and does not influence droplet collapse activity. A drop of water applied to a hydrophobic surface in the absence of surfactants (for example, fresh uninoculated MSB culture broth) will form a bead because the polar water molecules are repelled from the hydrophobic surface. However, if the water droplet contains surfactant, the force or interfacial tension between the water drop and the hydrophobic surface is reduced, which results in the spreading of the water drop over the hydrophobic surface.

For microplate assay, a 100 µl sample of the culture supernatant of 2,4-DNT grown cells was added into a well of a 96-mircowell plate. The plate was viewed using an underneath sheet of paper with a black and white grid. Presence of surfactant was confirmed by optical distortion of grid. If biosurfactant is present, the concave surface distorts the image of the grid below.

Drop collapse was performed according to the method of Jain *et al*.[13] and Hazra *et al*.[14] Briefly, lid of 96-microwell plate was coated with 2 ml of mineral oil and allowed to equilibrate for 1 h at 30 ^{o}C. Then 5 µl of culture supernatant of 2,4-DNT grown cells was added at the centre of the wells over the oil layer and the shape of the oil drop was visually inspected after 1 min. Biosurfactant-producing cultures give flat drops corresponding to partial to complete spreading on the oil surface. Those samples that give rounded drops are scored as negative indicative of the lack of surface activity.

For assaying emulsification activity, 2 ml of toluene was mixed with equal volume of cell-free supernatant of pre-grown culture in MSB (supplemented with 100 mg l^{-1} 2,4-DNT) in separate test tubes and vortexed at high speed for 2 min. Emulsification index (EI_{24}) was calculated by measuring the percentage of height occupied by the emulsion (stable cloudy appearance) after 24 h: [$\%EI_{24} = (h_{emulsion}/h_{total})\times100$].[15] Finally, surface tension of cell free broth was measured using a du Nouy ring tensiometer (DCA 315, Thermo Cahn, USA) having a resolution of 0.1 dyne cm^{-1}. The oil-displacement test with sunflower oil was done as described previously.[13] Surface tension was measured both for the culture grown in nutrient broth (NB) and for the culture grown on 2,4-DNT (100 mg l^{-1}) provided as sole source of carbon and energy in MSB media. After specific time intervals representative of mid of log growth phase and stationary phase, the culture broth was centrifuged at 10,000 rpm (Hereaus, Kendro Laboratory Products, Hanau, Germany) and 4 ^{o}C for 15 min. The

supernatant was filtered through 0.2 µm membrane filter and surface tension of the filtrate was measured.[16]

For the oil spreading technique, 40 ml of distilled water was added to a petri plate followed by addition of 20 µl of crude oil to the surface of the water. Then, 10 µl of cell-free supernatant of pre-grown culture in MSB (plus 100 mg l^{-1} 2,4-DNT) was carefully placed on the centre of the oil film. After 30 s of incubation, the diameter of clear halo zone was measured. If biosurfactant is present in the supernatant, the oil is displaced and a clearing zone is formed. The diameter of this clearing zone on the oil surface correlates to surfactant activity, also called oil displacement activity.[17]

Cell extracts preparation and enzyme assays

Cell extracts were prepared by resuspending cell pellets (obtained from a 100-ml culture of the strain grown on 2,4-DNT) in ice-cold 50 mM Tris-HCl buffer (pH 7.5) and sonicating them in an ice-water bath at 5.0-s on and 3.0-s off intervals for 10 min using a Vibracell sonic oscillator.[18] Cell debris was removed by centrifugation at 10,000 rev min^{-1} (Hereaus, Kendro Laboratory Products, Hanau, Germany) for 30 min at 4 °C. A clear supernatant was collected and used as an enzyme source.

For 2,4-DNT grown cells, nitroreductase activity was determined as per Yin *et al*.[19] Protein was determined by the method of Lowry *et al*.[20] using bovine serum albumin (BSA) as the standard. One unit of enzyme activity was defined as the amount required for catalyzing the formation or consumption of 1 µmol of product or substrate per minute. Electron transport system (ETS) activities of the 2,4-DNT-grown cells was measured as described previously.[21,22] The ETS activity (µmol g min^{-1}) was calculated as the formation of 1 µmol INT-formazan per minute using 1 g of the dry cell weight. Catalase (E.C. 1.11.1.6), glutathione-s-transferase (GST) (E.C. 2.5.1.18), and superoxide dismutase (E.C. 1.15.1.1)

activity was assayed as per Kulkarni *et al*.[23] The scavenging effect under 2,4-DNT stress in the strain for DPPH radical was estimated following the protocol of Kirankumar *et al*.[12]

Analysis of carotenoids

The total content of carotenoid accumulated in the cells was quantified following the method described earlier.[24] The carotenoid content of the extract was quantified by measuring the absorbance at a specific wavelength for γ-carotene (462 nm), lycopene (474 nm), β-carotene (454 nm), diapolycopene (470 nm), and diapotorulene (450 nm). The equation used to calculate the total carotenoid content is described elsewhere.[24,25]

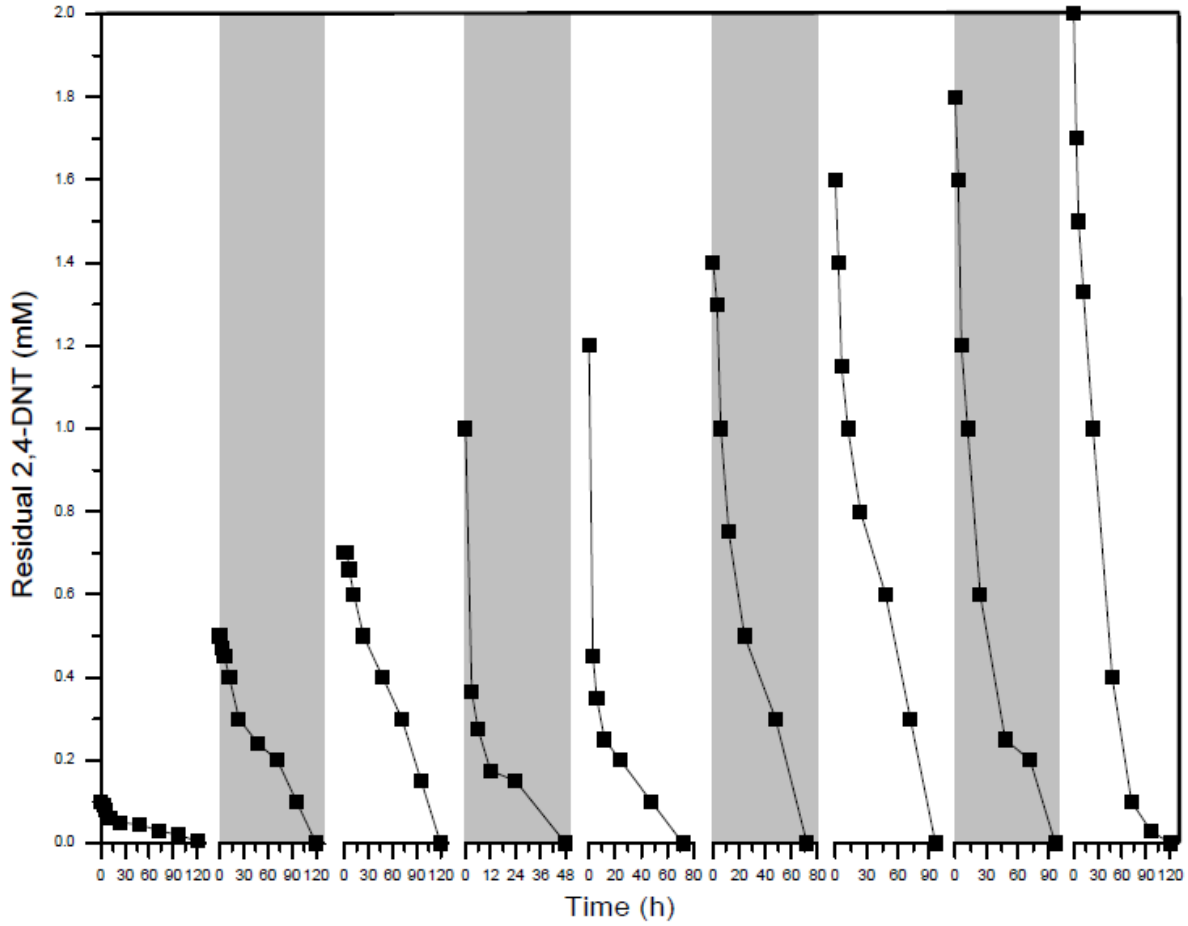

Fig. S1. Biodegradation of 2,4-DNT in MSB medium containing initial 0.1 mM 2,4-DNT and step by step transfer of cells into media containing increased concentration of 2,4-DNT during the acclimatization process.

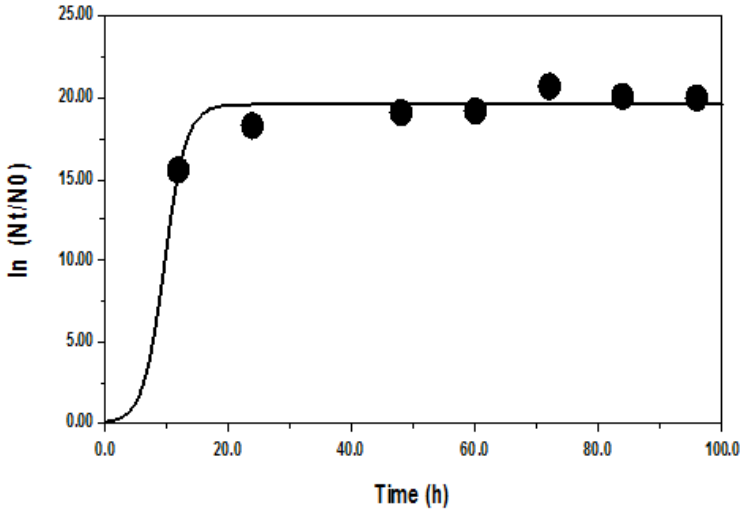

Fig. S2. Growth curve of strain NT2 fitted with logistic model at initial concentration of 100 mg l^{-1} of 2,4-DNT.

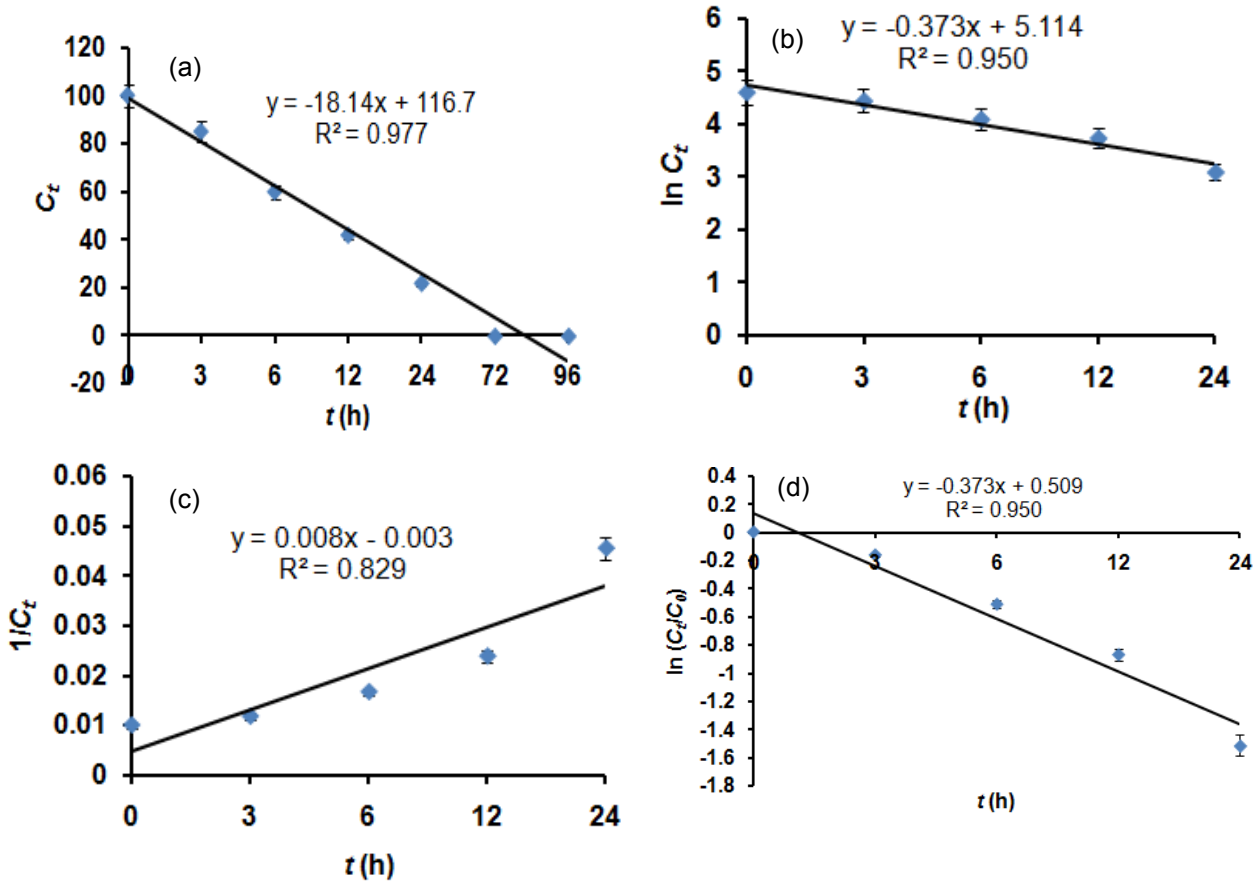

Fig. S3. Kinetic plots of (a) zero order, (b) first-order, (c) second-order and (d) pseudo-first order reaction model for 2,4-DNT (100 mg l^{-1}) degradation by strain NT2.

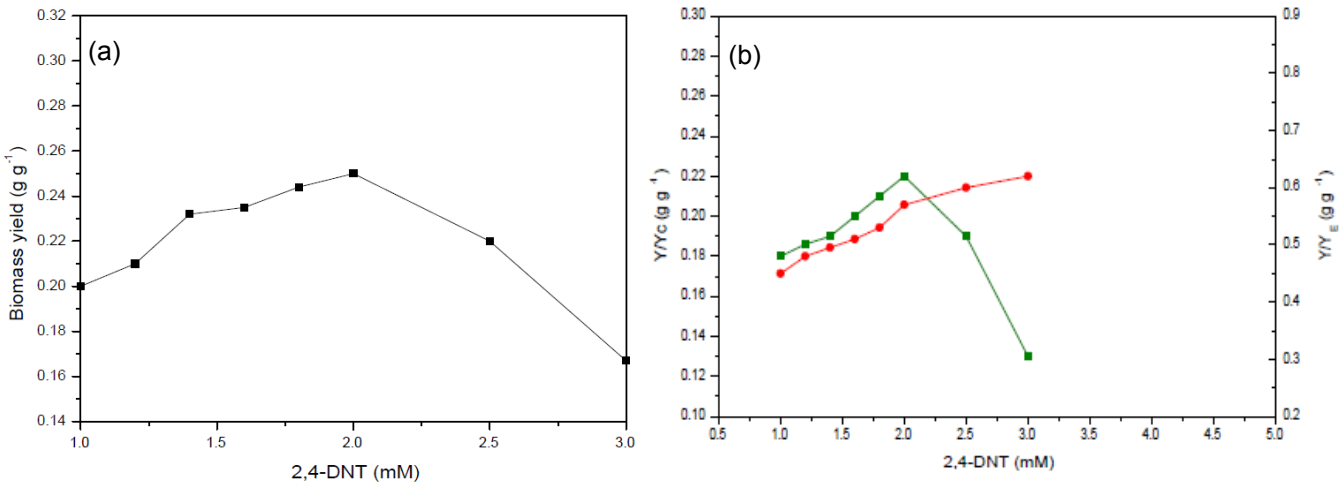

Fig. S4. Effect of 2,4-DNT on (a) cell mass yield and (b) the proportion of substrate carbon for cell biomass (■;Y/YC) and for energy (●;Y/YE). Values are the mean ± SD (n = 3).

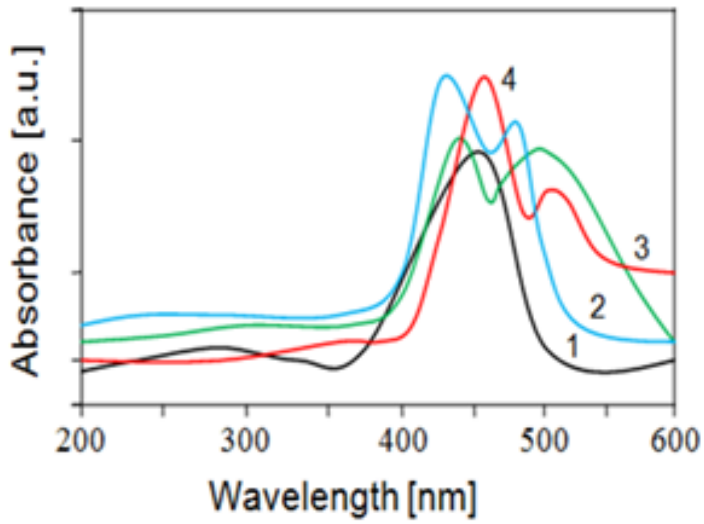

Fig. S5. UV-Vis spectra of orange colored carotenoids from *R. pyridinivorans* NT2 grown on 2,4-DNT.

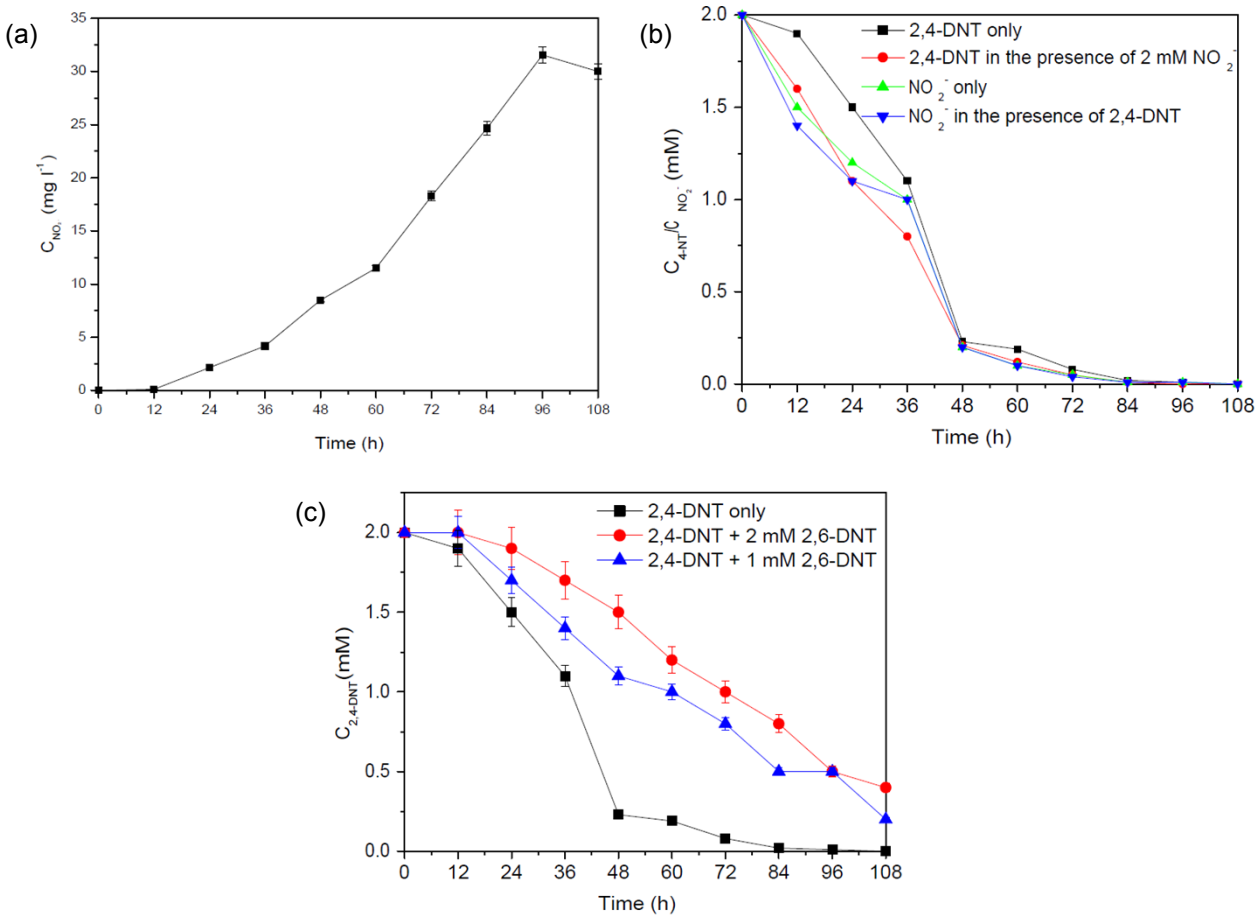

Fig. S6. (a) Accumulation of nitrite ions during biodegradation of 2,4-DNT by *R. pyridinivorans* NT2. (b) Uptake of 2,4-DNT in the presence/absence of NO_2^- and vice versa. (c) Uptake of 2,4-DNT from mixture with 1 and 2 mM 2,6-DNT.

Table S1. Two types of degradation rate during 2,4-DNT (gradually increased concentration) biodegradation

Initial concentration (mM)	Phase I[a]	Phase II[b]		Total[c]	
	Time (h)	Time (h)	Rate (mM h^{-1})	Time (h)	Rate (mM h^{-1})
2,4-DNT					
0.5	15	105	0.004	120	0.004
0.7	14	106	0.006	120	0.005
1.0	12	36	0.027	48	0.020
1.2	11	49	0.024	60	0.020
1.4	10	62	0.022	72	0.019
1.6	10	74	0.021	84	0.019
1.8	12	84	0.021	96	0.018
2.0	12	84	0.023	108	0.018

[a]Initial period during which less growth and degradation was observed; [b]Actual degradation period; [c]Whole degradation period

Table S2. Activity of nitroreductase during 2,4-DNT degradation

Stage of degradation	**Activity (Δabs min^{-1} mg^{-1} protein) at 400 nm**		
	0.5 mM	**1.0 mM**	**2.0 mM**
Before degradation	0.00	0.00	0.00
At initiation of degradation	1.88	2.33	2.11
At mid of degradation	2.14	2.54	2.28
Just after degradation	1.66	2.12	1.75

Table S3. Comparative analysis of total cellular fatty acids composition of strain NT2 grown on MSB media containing 2,4- DNT (2 mM)

Total Fatty acids	**0 h**	**72 h**
Total saturated fatty acids	53.96	71.88
Total unsaturated fatty acids	47.47	23.55
Total cyclo fatty acids	1.51	6.48
Total anteiso fatty acids	3.57	9.35
Total iso fatty acids	3.21	7.27

Values are represented as percentage of total fatty acids

The average error associated with the GC-FID quantification of each FAME was ±3.5 %, quoted for a confidence interval of 99 %

Table S4. Effect of 2,4-DNT (2 mM) on cellular growth, shape, and ratio between cell surface and volume of strain NT2

Compound	Length (µm)	Width (µm)	Radius (µm)	Surface area (μm^2)	Volume (μm^3)	Surface/volume
2,4-DNT						
0 h	0.783	0.455	0.227	1.765	0.176	10.028
12 h	1.158	0.572	0.286	2.138	0.394	5.406
24 h	1.685	0.523	0.2125	3.322	0.420	7.909
72 h	2.052	0.502	0.210	3.784	0.460	8.226

Table S5. Profile of oxidative stress enzymes and reactive oxygen species monitored during growth and degradation of 2,4-DNT (2 mM) in MSB media by strain NT2

Antioxidant enzymes	**0 h**	**72 h**
Catalase (mM min^{-1}mg $protein^{-1}$)	0.13±0.08	0.29±0.5*
Superoxide dismutase (U min^{-1}mg $protein^{-1}$)	1.1±0.3	11.5±2.7**
Glutathione S-transferase (mM min^{-1}mg $protein^{-1}$)	2.15±0.24	5.07±0.01*
DPPH radical scavenging (%)	6	18.5***

Data are mean ± S.D. Means are compared with unpaired t-test using Origin v6.1 software

*P<0.05; **P<0.01; ***P<0.001 (Significantly different when compared with respective control, i.e. 0 h)

Table S6: Comparison of 2,4-DNT transformation with previous literature data

Candidates	Electron donor	Electron acceptor	pH	Maximum concentration (mM) degraded	Transformation efficiency	Time required	Refs.
Microorganism							
Pseudomonas sp.	2,4-DNT	Oxygen	7.0	0.54	100%	120 h	26
Microbial community	Ethanol	2,4-DNT	-	0.02	100%	32 d	27
Microbial consortia	2,4-DNT	Oxygen	6.8	0.25	100%	73 h	28
Phanerochaete chrysosporium	Glucose	2,4-DNT	-	0.25	100%	6 d	29
P. aeruginosa	Ethanol	2,4-DNT	6.5-7.8	0.25	100%	13 d	30
Lactococcus lactis subsp. *lactis*	Glucose	2,4-DNT	-	0.17	100%	12 h	31
Microbial community	Ethanol	2,4-DNT	7.2	0.08	100%	120 h	32
Clostridium acetobutylicum	Saccharides	2,4-DNT	7.0	0.54	100%	1 h	33
Pseudomonas putida OU83	-	Oxygen	7.5	0.4	98%	48 h	34
Microbial community	-	-	-	13.5	66%	50 d	35
Pseudomonas putida NDT1	2,4-DNT	Oxygen	7.0	0.054	100%	15 d	36
Microbial community	-	-	-	1.51	99%	15 d	37
Microbial community	Ethanol	2,4-DNT	-	0.054	99%	150 d	38
S. oneidensis MR-1	Lactate	2,4-DNT	7.0	0.09	100%	24 h	39
Arthrobacter sp. K1	2,4-DNT	Oxygen	7.0	0.47	66%	10 d	40
S. marisflavi EP1	Lactate	2,4-DNT	7.0	0.2	100%	24 h	41
R. pyridinivorans NT2	2,4-DNT	Oxygen	7.0	2	100%	108 h	This study
Plants							
Hemp, flax, sunflower, mustard	-	-	-	1.08	100%	3 d	42
Chemical catalysts							

Ozone	-	-	-	13.5	70%	100 d	43
n-Hexane soot	Dithiothreitol	2,4-DNT	7.4	0.18	100%	7 d	44
Fe^0	-	-	7.0	1.35	70%	5 d	45

Table S7: Comparison of degradation of 2,4-DNT

Culture	**% degradation**
R. pyridinivorans NT2	98.22±1.66
R. pyridinivorans cured derivative	13.11±2.05
Transformant *E. coli* DH5α	76.33±1.52
E. coli DH5α	4.50±1.92

Table S8: Antibiotic resistance profile of NT2, DH5α and transformed DH5α

Antibiotics used	***R. pyridinivorans* NT2**		***E. coli* DH5α**		**Transformed *E. coli* DH5α**	
	Zone of inhibition	**Result**	**Zone of inhibition**	**Result**	**Zone of inhibition**	**Result**
Amikacin (30 µg)	23 mm	S	26 mm	S	24 mm	S
Chloramphenicol (10 µg)	21 mm	S	23 mm	S	23 mm	S
Erythromycin (15 µg)	5 mm	R	22 mm	S	5 mm	R
Gentamicin (30 µg)	25 mm	S	23 mm	S	25 mm	S
Tetracycline (30 µg)	8 mm	R	17 mm	IS	8 mm	R

S, sensitive; R, resistant; IS, Intermediate sensitive

References

1 K.K. Kovari, T. Elgim, *Microbiol. Mol. Biol. Rev.*, 1998, **62**, 646-666.

2 K. Han, O. Levenspiel, *Biotechnol. Bioeng.*, 1988, **32**, 430-437.

3 G.C. Okpokwasili, C.O. Nweke, *African J. Biotechnol.*, 2005, **5**, 305-317.

4 V.H. Edwards, *Biotechnol. Bioeng.*, 1970, **12**, 679-712.

5 M. Wayman, M.C. Tseng, *Biotechnol. Bioeng.*, 1976, **18**, 383-387.

6 G. Alagappan, R.M. Cowan, *Biotechnol. Bioeng.*, 2001, **75**, 393-405.

7 N.-C. Choi, J.-W. Choi, S.-B. Kim, D.-J. Kim, *Appl. Microbiol. Biotechnol.*, 2008, **81**, 135-141.

8 A. Kumar, S. Kumar, S. Kumar, *Biochem. Eng. J.*, 2005, **22**, 151-159.

9 A. Rajan, N. Aruna, S. Kaur, *Biotechnol. Bioinf. Bioeng*., 2011, **1(3)**, 319-323

10 G. Neumann, Y. Veeranagouda, T.B. Karegoudar, O¨. Sahin, I. Ma¨usezahl, N. Kabelitz, U. Kappelmeyer, H.J. Heipieper, *Extremophiles*, 2005, **9**, 163-168.

11 Y. Veeranagouda, T.B. Karegoudar, G. Neumann, H.J. Heipieper, *FEMS Microbiol. Lett.*, 2006, **254**, 48-54.

12 B. Kirankumar, B.K. Guruprasad, M. Santoshkumar, S.N. Anand, T.B. Karegoudar, *Extremophiles*, 2013, **17**, 1037-1044.

13 D.K. Jain, D.L. Collins-Thompson, H. Lee, J.T. Trevors, *J. Microbiol. Methods* 1991, **13**, 271-279.

14 C. Hazra, D. Kundu, A. Chaudhari, *RSC Adv*., 2015, **5(4)**, 2974-2982.

15 C.Y. Chen, S.C. Baker, R.C. Darton, *J. Microbiol. Methods* 2007, **70(3)**, 503-510.

16 I. Ghosh, J. Jasmine, S. Mukherji, *Bioresour. Technol*., 2014, **166**, 548-558.

17 N.H. Youssef, K.E. Duncan, D.P. Nagle, K.N. Savage, R.M. Knapp, M.J. McInerney, *J. Microbiol. Methods* 2004, **56(3)**, 339-347.

18 X.-J. Tian, X.-Y. Liu, H. Liu, S.-J. Wang, N.-Y. Zhou, *Appl. Microbiol. Biotechnol*.,

2013, **97**, 9217-9223.

19 Y. Yin, Y. Xiao, H.-Z. Liu, F. Hao, S. Rayner, H. Tang, N.-Y. Zhou, *Appl. Microbiol. Biotechnol.*, 2010, **87**, 2077-2085.

20 O.H. Lowry, N.J. Rosebrough, A.L. Farr, R.J. Randall, *J. Biol. Chem*., 1951, **192**, 265-275.

21 J.J. Smith, G.A. McFeters, *J. Microbiol. Methods* 1997, **29**, 161-175.

22 F. Li, L. Zhu, *Bioresour. Technol*., 2012, **123**, 42-48.

23 S.V. Kulkarni, V.L. Markad, J.S. Melo, S.F. D'Souza, K.M. Kodam, *Appl. Microbiol. Biotechnol*., 2014, **98**, 919-929.

24 J.R. Kim, M.K. Kong, S.Y. Lee, P.C. Lee, *World J. Microbiol. Biotechnol*., 2010, **26**, 2231-2239.

25 J.H. Kim, S.H. Kim, J.H. Yoon, P.C. Lee, *Appl. Microbiol. Biotechnol*., 2014, **98**, 3759-3768.

26 R.J. Spanggord, J.C. Spain, S.F. Nishino, K.E. Mortelmans, *Appl. Environ. Microbiol*., 1991, **57**, 3200-3205.

27 H.J. Christopher, 1998, M. Sc. Thesis, Virginia Polytechnic Institute and State University, Virginia.

28 Z. Snellix, A. Nepovím, S. Taghavi, J. Vangronsveld, T. Vanek, D. van der Lelie, *Environ. Sci. Pollut. Res*., 2002, **9**, 48-61.

29 K. Valli, B. J. Brock, D.K. Joshi, M. H. Gold, *Appl. Environ. Microbiol*., 1992, **58(1)**, 221-228.

30 D.R. Noguera, D.L. Freedman, *Appl. Environ. Microbiol*., 1996, **62**, 2257-2263.

31 K.-H. Shin, Y. Lim, J.-H. Ahn, J. Khil, C.-J. Cha, H.-G. Hur, 2005, *Chemosphere*, **61**, 30-39.

32 J. Cheng, M.T. Suidan, A.D. Venosa, *Water Res*., 1998, **32**, 2921-2930.

33 J.B. Hughes, C.Y. Wang, C.L. Zhang, *Environ. Sci. Technol*., 1999, **33**, 1065-1070.

34 S.K. Walia, S. Ali-Sadat, R. Brar, G.R. Chaudhry, *Pestic. Biochem. Physiol*., 2002, **73**, 131-139.

35 D. Cassidy, A. Northup, D. Hampton, *J. Chem. Technol. Biotechnol*., 2009, **84**, 820-826.

36 T. Hudcova, M. Halecky, E. Kozliak, M. Stiborova, Jan Paca, *J. Hazard. Mater*., 2011, **192**, 605-613.

37 Ö.S. Kuşçu, D.T. Sponza, *J. Hazard. Mater*., 2011, **187**, 222-234.

38 Z.-Y. Wang, Z.-F. Ye, M.-H. Zhang, *J. Appl. Microbiol*., 2011, **110**, 1476-1484.

39 J. Huang, X. Cheng, F. Li, G.D. Sheng, *Microbiol. China*, 2013, **40**, 1734-1741.

40 P. Küce, G. Coral, Ç. Kantar, *Ann. Microbiol*., 2014, DOI 10.1007/s13213-014-0880-5.

41 J. Huang, G. Ning, F. Li, G.D. Sheng, *Biores. Technol*., 2015, **180**, 200-206.

42 R. Podlipná, B. Pospíšilová, T. Vaněk, *Ecotox. Environ. Safe*., 2015, **112**, 54-59.

43 D. Cassidy, A. Northup, D. Hampton, *J. Chem. Technol. Biotechnol*., 2009, **84**, 820-826.

44 S.Y. Oh, P.C. Chiu, *Environ. Sci. Technol*., 2009, **43**, 6383-6388.

45 J.H. Fan, H.W. Wang, D.L. Wu, L.M. Ma, *J. Chem. Technol. Biotechnol*., 2010, **85(8)**, 1117-1121.